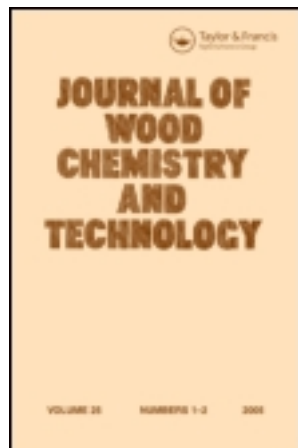


This article was downloaded by: [Southeast University]

On: 18 January 2014, At: 02:10

Publisher: Taylor & Francis

Informa Ltd Registered in England and Wales Registered Number: 1072954 Registered office: Mortimer House, 37-41 Mortimer Street, London W1T 3JH, UK



Journal of Wood Chemistry and Technology

Publication details, including instructions for authors and subscription information:

<http://www.tandfonline.com/loi/lwct20>

The Microstructure of Paper after Heat-Induced Inkless Eco-Printing and its Features

Jinxiang Chen^a, Juan Xie^a, Le Pan^a, Xin Wang^a, Lina Xu^b & Yun Lu^c

^a International Institute for Urban Systems Engineering & School of Civil Engineering, Southeast University, Nanjing, China

^b State Key Laboratory of Bioelectronics, Jiangsu Laboratory for Biomaterials and Devices, School of Biological Science and Medical Engineering, Southeast University, Nanjing, China

^c Department of Mechanical Engineering, Graduate School & Faculty of Engineering, Chiba University, Chiba, Japan

Published online: 10 Jan 2014.

To cite this article: Jinxiang Chen, Juan Xie, Le Pan, Xin Wang, Lina Xu & Yun Lu (2014) The Microstructure of Paper after Heat-Induced Inkless Eco-Printing and its Features, Journal of Wood Chemistry and Technology, 34:3, 202-211

To link to this article: <http://dx.doi.org/10.1080/02773813.2013.853085>

PLEASE SCROLL DOWN FOR ARTICLE

Taylor & Francis makes every effort to ensure the accuracy of all the information (the "Content") contained in the publications on our platform. However, Taylor & Francis, our agents, and our licensors make no representations or warranties whatsoever as to the accuracy, completeness, or suitability for any purpose of the Content. Any opinions and views expressed in this publication are the opinions and views of the authors, and are not the views of or endorsed by Taylor & Francis. The accuracy of the Content should not be relied upon and should be independently verified with primary sources of information. Taylor and Francis shall not be liable for any losses, actions, claims, proceedings, demands, costs, expenses, damages, and other liabilities whatsoever or howsoever caused arising directly or indirectly in connection with, in relation to or arising out of the use of the Content.

This article may be used for research, teaching, and private study purposes. Any substantial or systematic reproduction, redistribution, reselling, loan, sub-licensing, systematic supply, or distribution in any form to anyone is expressly forbidden. Terms &

Conditions of access and use can be found at <http://www.tandfonline.com/page/terms-and-conditions>

The Microstructure of Paper after Heat-Induced Inkless Eco-Printing and its Features

JINXIANG CHEN,¹ JUAN XIE,¹ LE PAN,¹ XIN WANG,¹
LINA XU,² AND YUN LU³

¹International Institute for Urban Systems Engineering & School of Civil Engineering, Southeast University, Nanjing, China

²State Key Laboratory of Bioelectronics, Jiangsu Laboratory for Biomaterials and Devices, School of Biological Science and Medical Engineering, Southeast University, Nanjing, China

³Department of Mechanical Engineering, Graduate School & Faculty of Engineering, Chiba University, Chiba, Japan

Abstract: *Microstructural changes in paper after heat-induced inkless eco-printing (HIEP) and pyrolysis productions of paper were investigated by scanning electron microscopy and pyrolysis-gas chromatography/mass spectrometry (Py-G/MS). The results were as follows: (1) When the heat-induced temperature is between 350°C and 600°C, slight scratches are left on the paper surface after scan printing, but click printing leaves obvious concave indentations. Both of these printing methods can create a clear and clean boundary with no significant carbonized microstructure. (2) Experimental studies show that paper undergoes true pyrolysis at 500°C. The simulated printing test shows that the fibers on the paper surface exhibit a yellow discoloration that meets printing requirements. (3) Compared with current laser printing techniques and laser inkless eco-printing (LIEP), HIEP has the advantages of avoiding the de-inking process during paper recycling and preserving paper strength better than LIEP.*

Keywords HIEP, inkless printing, SEM microscopy, paper pyrolysis, zink, microstructure

Introduction

Current laser and ink-jet printers produce harmful gases that pollute the environment. This adds to regeneration costs and reduced paper quality. In recent years, researchers in the printing industry have studied ecological inkless print technology (also called inkless, zero ink, or zink). Thus far, except for inkless laser carbonized^[1, 2] printing technology, these technologies rely on particular features of the printing paper. For example, ZINK Imaging Inc.^[3] produces a printing technology in which the heat produced through printing causes a large number of crystal dyes contained in the printing paper to change into a

This work was supported by the Peak of Six Personnel in Jiangsu Province (No. 2012-JNHB-013).

Address correspondence to Jinxiang Chen, International Institute for Urban Systems Engineering & School of Civil Engineering, Southeast University, 2#, Sipailou, Nanjing210096, China. E-mail: chenpaper@yahoo.co.jp

variety of colors; the same company also invented the Pandigital inkless printer.^[4] Dell Inc. created the Wasabi PZ310 mini-printer based on the principle that a special coating layer on the photographic paper can reflect different wavelengths of light to produce a photo. Dell's technology also employs the nano-structural changes of a special substance on the surface layer^[5,6,7] or a liquid polymer^[8] in the printing process. Moreover, the use of natural pigments^[9,10,11] with ordinary printing paper represents another type of eco-printing technology. For survival purposes, organisms in nature have adapted to their environments throughout history via a process called evolution, and this process often results in the development of specialized structures with specific functions. Bionic innovations take their inspiration from these natural structures.^[12,13] Recently, inspired by the yellowing discoloration^[14,15] of plant fibers, the authors proposed a radically new concept of heat-induced inkless eco-printing (HIEP)^[16] that does not require ink during the printing process and can achieve the same printing results using an ordinary sheet of office paper. We previously discussed the mechanism that allows for negligible damage of paper during HIEP.^[17] This paper focuses on the microstructure of paper after HIEP, paper pyrolysis products, and the advantages of HIEP.

Experimental Methods

Heat-Induced Color Blocks and Simulated Printing Experiments

Hoopoe[®] office paper (A4, 70 g/mm², white, Dadong Pulp & Paper) was used in this study, and its major ingredients are cellulose 62%, hemicellulose 10%, ash (filler) 12%, and water 7%.^[17] To fabricate heat-induced color blocks, a wide ironing (Figure 1a) head was applied by touching and sliding over the paper and was operated by hand with a certain speed at room temperature. The experimental temperatures were set to 350°C, 400°C, 450°C, and 480°C. Using this method, color blocks approximately 7 mm wide by 8 mm long were drawn at each temperature, as shown in Figure 1b. Small heat-induced points were produced on the paper using the click printing method at 480°C and 600°C with the devices shown in Figures 1a (tip-head) and 1c, respectively.

Microstructure Observation

After simulated printing with HIEP and a current laser printer, paper microstructures were observed with an Ultra Plus Field Emission Scanning Electron Microscope (FE-SEM; Carl Zeiss NTS GmbH, Oberkochen, Germany).

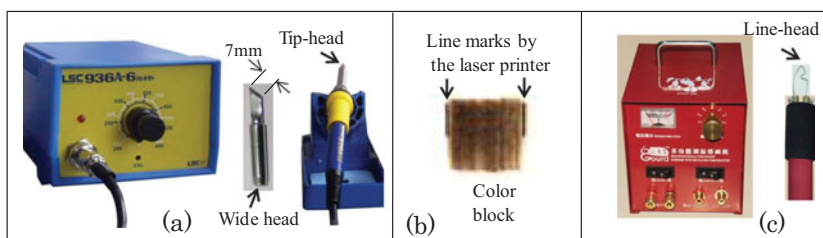


Figure 1. The controller and the shape of its head for two electric soldering irons (a, c), and a sample of the color block (b) (color figure available online).

Experimental Analysis of Py-GC/MS

The gas chromatography (GC) conditions were as follows: DB-5 column, helium (carrier gas), column flux 0.9 mL/min, split ratio 100:1; column temperature rise progress: maintain initial temperature -40°C for 3 min, then ramp up to 300°C at a rate of $15^{\circ}\text{C}/\text{min}$, and maintain for 5 min. The mass spectrometry (MS) conditions were as follows: EI ionization sources, 200°C , electron energy 70 eV, electron bombardment, full-scan mode, quality scan range (m/z) 15–500.

The samples were placed in a platinum boat, which was then dropped into a quartz pyrolysis tube in free-fall style. Pyrolysis products were separated and identified by combined GC-MS (Simazu 2010). The pyrolysis temperature was 500°C , (pyrolysis time: approximately 0.1 s), and the Mist spectral library search and normalization method was used to calculate the peak areas.

Experimental Results and Discussion

Carbonized Microstructure of the Paper after HIEP and Features of HIEP

Figures 2a and 2b show contrast photographs of the paper before HIEP. Figures 2c-h show a set of microstructure images. The images in the left correspond to simulated scan printing, and those on the right are samples of click printing. Each row represents samples printed at the same temperature. As reported in a previous paper,^[17] cellulose and hemicellulose are the major ingredients in the original paper (before HIEP), and the mutual superposition of fibers leads to the formation of many recesses and voids (Figure 2, with the letter “v”). It has been reported that the porosity of the paper is typically up to 50%.^[18] Thus, many intact fibers can be observed in Figures 2a and 2b, as indicated by wide arrow marks. A number of particles or slightly larger lumps can also be observed in the images in Figure 2, as indicated by the square marks. Most of these substances are inorganics (filler or addition agents) added during the papermaking process, which are usually sorted as “ash.” The ash content of the measured experimental sample was approximately 12%.^[17] However, as shown in the microstructure (Figures 2c-h), slight scratches are left on the paper surface after scan printing (Figure 2, indicated by a “w”), but very obvious concave indentations are left after click printing (Figure 2, indicated by a “u”). Following treatment at different temperatures, the microstructures differ in appearance. After click printing, the fibers on the surface of the concave indentations seem more flat (Figures 2f and 2h, indicated by a broad arrow mark) or even crushed (Figures 2f and 2h, indicated with an asterisk). Meanwhile, the ash particulate matter increased slightly (Figures 2f and 2h, indicated with the square mark), but not in an obvious manner. For scan printing, a similar phenomenon was observed, including deeper scratches with increasing temperature, but the differences between various temperatures were not obvious (Figure 2).

The images in Figures 3a-d from the LIEP paper are provided for comparison purposes. The white dotted lines divide the LIEP and the non-heat printing samples, and the side of the letter “P” (as marked) is printed. Figure 4 shows SEM images of the microstructures after current laser printing. As shown in Figures 3a and 3b, in addition to the fiber, a number of small holes (circle marks) and cauliflower core-like clots (triangle marks) can be clearly observed after LIEP. The surface of the material resembles microsludge, with a texture similar to that of a softening substance generated by fiber carbonation decomposition. It is known that the carbonization is a final step in thermal degradation (pyrolysis) of cellulose or hemicelluloses. However, it is processed by other steps, including depolymerization of them,

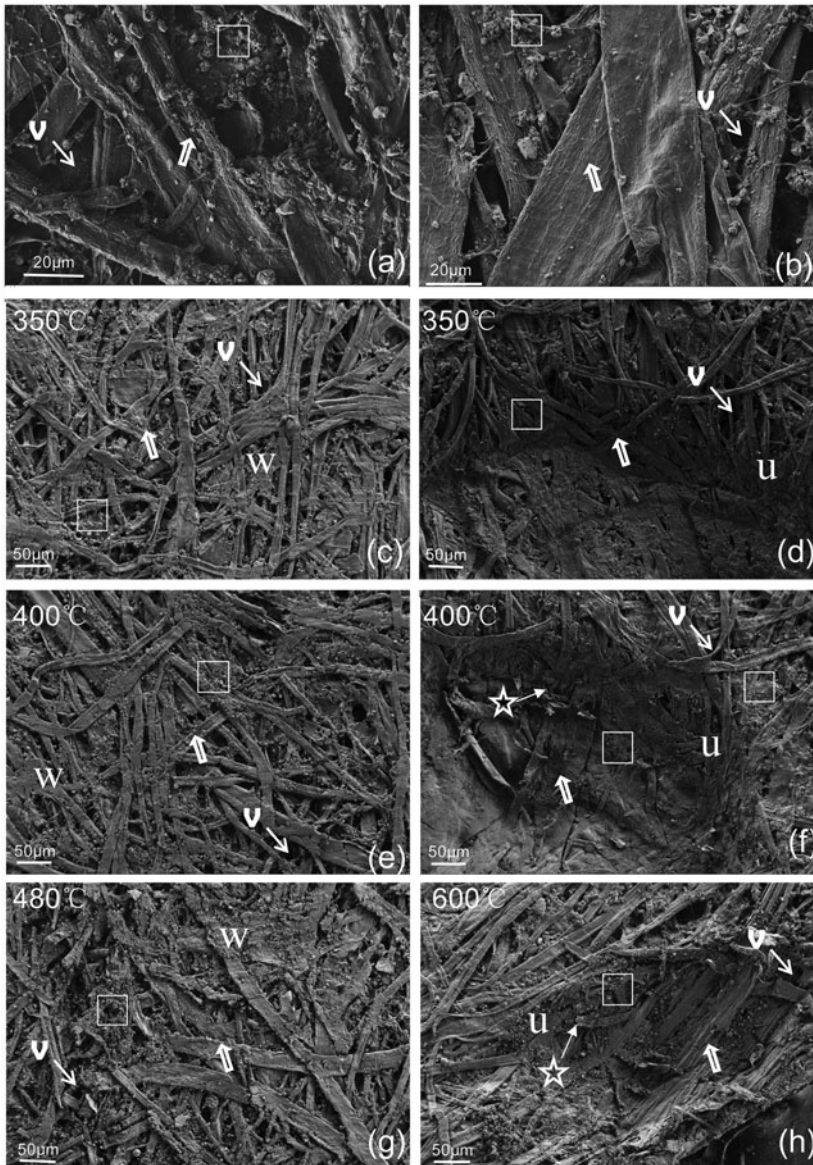


Figure 2. The microstructure of paper after HIEP. (a, b) Control samples; (c, e, g) scan printing samples; (d, f, h) click printing samples. The broad arrow: the fiber; the square: the ash; the letter “w” the slight scratches; the “u”: the concave; the letter “v”: an irregular void. The asterisk: the fiber fragment.

formation of levoglucosan, and chromophore formation. The laser-induced changes derive mainly from local heating of the sample under the focused beam. Therefore, the surface layer on the paper has been carbonized because the paper is subjected to concentrated laser energy with LIEP (Figure 3). With HIEP, the changes of the paper were only stopped on the initial steps, such as depolymerization of cellulose or hemicellulose, formation of levoglucosan, and chromophore formation. Thus, compared with the carbonation phenomenon occurring during LIEP, HIEP maintains sufficient paper strength with no obvious carbonation.

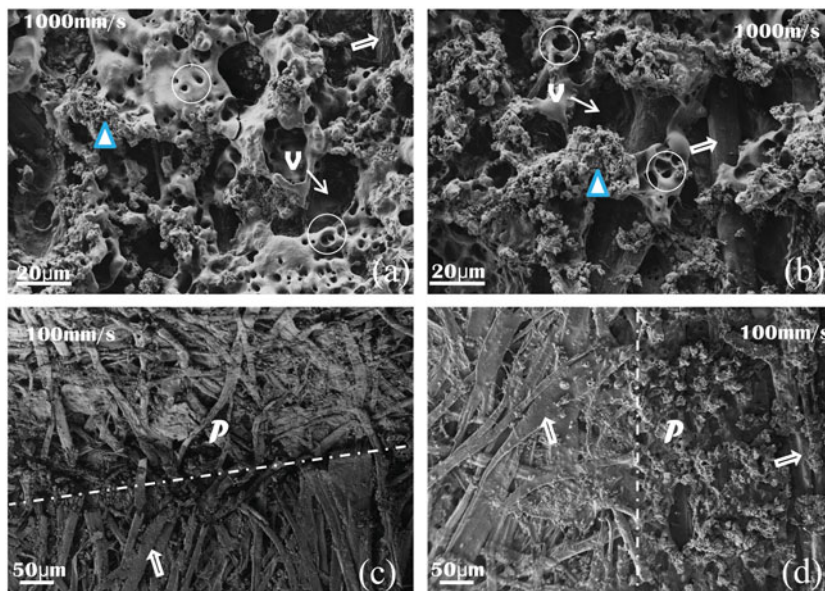


Figure 3. Microstructure of the printing paper in text areas after LIEP. (a, b) Two typical carbonation structures; (c, d) the boundary structure. The white dotted lines indicate the division between LIEP and non-LIEP; the letter “P”: the side after LIEP. The broad arrow: the fiber; the circle: the small holes; the triangle: the cauliflower core-like clots; the letter “v”: the irregular void (color figure available online).

As shown in Figures 3c and 3d, both of the LIEP photographs have a clear and relatively clean dividing line. With current laser printing (Figure 4), the paper surface adsorbs a lot of ink powder, making the thickness greater in the middle of the text but smaller at the edge. The boundaries are unevenly jagged and are influenced by the fiber distribution in the paper. Therefore, based on the investigation of physical changes in the concave and protruding lesions (Figure 2, indicated by “w” and “u” marks), it is clear that, in the simulated HIEP samples, including both scan printing and click printing, boundaries were formed in a manner similar to ecological and current laser printing. The pigments in the printed areas

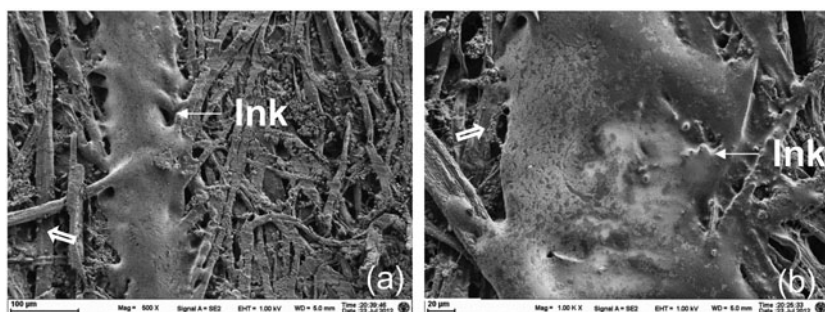
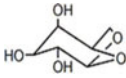
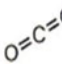

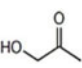
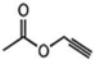
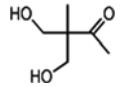
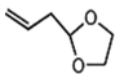


Figure 4. Microstructure of the paper surface after current laser printing. Low-magnification photographs; (b) high-magnification photographs. The broad arrow: the fiber.

Table 1
Main pyrolysis products at 500°C*

Time(min)	17.38	1.75	8.47	4.69	6.11	3.26	12.49
	Levoglucosan	Carbon dioxide	α -Angelica lactone	Acetol	Propargyl acetate	3,3-bis (hydroxymethyl)-2-Butanone	2-Allyl-1,3-dioxolane
Formula	$C_6H_{10}O_5$	CO_2	$C_5H_6O_2$	$C_3H_6O_2$	$C_5H_6O_2$	$C_6H_{12}O_3$	$C_6H_{10}O_2$
Area%	30.80	23.38	10.54	8.40	5.22	4.71	3.42
Molecular structure							

*Major ingredients of the paper include cellulose 62%, hemicellulose 10%, ash (filler) 12%, and water 7%.

are not produced by physical changes, but by yellowing discoloration generated by the heat action of paper fibers.

Discussion of Paper Pyrolysis Products and Printing Features

HIEP differs from LIEP in that it produces no obvious carbonized microstructures. How can the fibers on the paper surface have a yellow discoloration without carbonization occurring during HIEP? Pyrolysis treatment conducted for 0.1 s at 500°C revealed the mechanism (Table 1). The main components of the printing paper are cellulose and hemicellulose (the structural formulas are listed in Figure 5).^[19–22] There have been many reports^[23–25] on converting biomass into bio-oil faster and more efficiently,^[26,27,28] including biomass pyrolysis,^[29,30,31] weight loss caused by heat,^[14,32,33] and the associated carbonation mechanism. Although the purpose of HIEP is unrelated to the conversion of biomass, the aims of reducing weight loss (pyrolysis) as much as possible and producing yellow discoloration are important for printing. The previous results can be used in the following discussion.

As mentioned above, although no obvious carbonized structures are present in the SEM images of the HIEP samples, more than 20 types of pyrolysis products were detected in the mass spectrometry experiments. As shown in Table 1, the two main pyrolysis products are levoglucosan and carbon dioxide, which account for more than 50% of the total pyrolysis mass spectrometry area. Seven of the substances in Table 1 account for up to 86% of the area. This means that the major pyrolysis product is levoglucosan, which is consistent with Wu's report^[34] showing that the relative content of levoglucosan in the pyrolysis products of

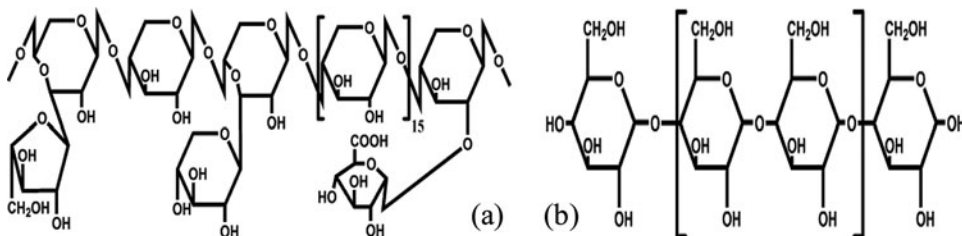


Figure 5. Molecule structures of hemicellulose (a) and cellulose (b).^[22]

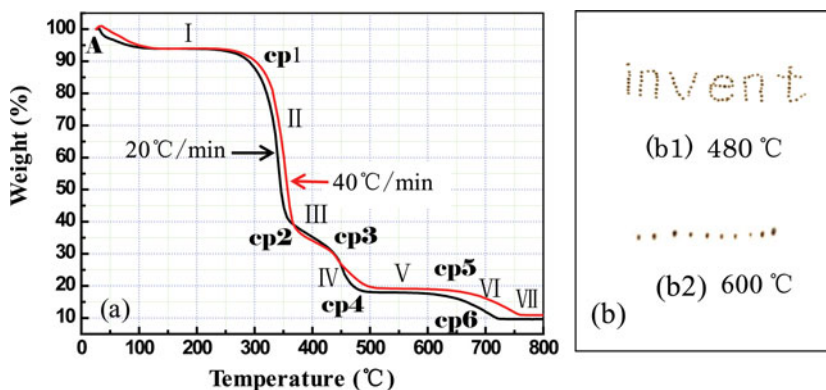


Figure 6. TG curves (a) and printing effects (b) (color figure available online).

cellulose is 61% at 400 °C and 23% at 550 °C. According to Wu,^[34] hemicellulose pyrolysis causes side-chain removal, macromolecule chain depolymerization, and intermolecular dehydration polymerization, in that order. Cellulose is a chain macromolecule compound composed of D-glucose linked by glycosidic bonds. Macromolecule chain depolymerization first occurs during pyrolysis. Levoglucosan is formed by cellulose macromolecules after the β -(1, 4) glycosidic bonds are cleaved and the monomers undergo intermolecular rearrangement. Ketones such as 2-butanone and 1-hydroxyl-2-propanone are formed by the C2 and C3 in the glucose monomers after intermolecular bond breaking and the hemiacetal group ring opening.^[34]

The structural formulas of pyrolysis products for hemicellulose and cellulose (Figure 5) are shown in Table 1. The following direct visual observations were made: except for carbon dioxide, the pyrolysis products are mostly carbohydrates with five or six carbon atoms. During heat induction, cellulose main chains are cut off directly or are simply reorganized. Carbon dioxide itself is the fractionlet formed during pyrolysis of the side groups or main chains.

Figures 6a and 6b show the experimental weight loss curves (TG) of printing paper and simulated click printing samples, respectively.^[16,17] Combined with the previous research results,^[17] these data indicate that the paper undergoes no significant damage during HIEP when the heat-induced temperature is 600 °C. The amount of heat transferred differs by at least two orders of magnitude between HIEP and the TG experiment (Figure 6a). The buffering effect of water (>5%) due to evaporation prevents damage to the paper. During heat induction, unlike in LIEP, the paper is not subjected to concentrated laser energy. Thus, although the temperature reaches 600 °C, there is no significant carbonization at the macro level. Compared with LIEP, the HIEP technology maintains better paper strength. The TG curves (Figure 6a), the previously reported results from Wu, and particularly the mass spectrum analysis results of this study demonstrate that the paper indeed decomposes at the high temperature in HIEP. The simulated printing (Figure 6b) and chromatography determination^[16] results confirm that HIEP can meet printing requirements.

In addition, harmful substances are emitted from toner or ink during current laser printing (Figure 4), and significant carbonization appears on the printing paper surface during LIEP. The HIEP process, in contrast, does not consume toner or ink, does not require an ink supply unit, and does not cause carbonization. Thus, HIEP technology significantly reduces waste paper recycling costs associated with ink processing, and its use carries excellent economic and environmental benefits.

In conclusion, we have analyzed the microstructure of printed paper and the yellow fiber discoloration that occurs without carbonization during HIEP. Going forward, the detailed mechanism of HIEP requires further study. The substance that forms during the decomposition process needs to be identified, and its content and toxicity, as well as its effect on the yellow discoloration, need to be determined.

Conclusions

This paper discussed the microstructure of paper, the pyrolysis products formed during HIEP, and the features of printing with HIEP. We have drawn the following conclusions:

1. When the printing temperature is between 350°C and 600°C, slight scratches are left on the paper surface after scan printing, and obvious concave indentations are left after click printing. Both of these printing methods produce a clear and clean boundary with no significant carbonized microstructure.
2. After pyrolysis for approximately 0.1 s at 500°C, the main pyrolysis products in the paper are laevoglucose and carbon dioxide. The simulated printing test showed that when the pyrolysis temperature is between 400°C and 600°C, the fibers on the paper surface have a yellow discoloration that meets printing requirements.
3. Compared with current laser printing methods and LIEP, HIEP technology has the advantages of avoiding de-inking during paper recycling and maintaining better paper strength.

References

1. Yao, N.M.; Zhao, X.L. Printing paper carbonization method with laser high temperature, ZL, **2007**, 200710071837.5 (in Chinese).
2. Sun, X.L.; Zhao, Z.; Bai, Z. A new no ink laser printing technology. *Mechatronics* **2009**, *12*, 84–86. (in Chinese)
3. Ferraro, P.; Coppola, S.; Grilli, S.; Paturzo, M.; Vespini, V. Dispensing nano-pico droplets and liquid patterning by pyroelectrodynamical shooting. *Nat. Nanotechnol.* **2010**, *5*, 429–35.
4. Song, X.M.; Wang, S.L. Simple analysis about inkless printing technology. *Publishing and Printing* **2010**, *3*, 44 (in Chinese).
5. Shestopalov, A.A.; Clark, R.L.; Toone, E.J. Inkless microcontact printing on self-assembled monolayers of FMOC-protected aminothiols. *J. Am. Chem. Soc.* **2007**, *129*(45), 13818–13819.
6. Choi, S.J.; Park, J.Y. High-aspect-ratio imageable top-surface lithography using UV-assisted inkless contact printing. *Small* **2010**, *6*(3), 371–375.
7. Shestopalov, A.A.; Clark, R.L.; Toone, E.J. Catalytic microcontact printing on chemically functionalized H-terminated silicon. *Langmuir* **2010**, *26*(3), 1449–1451.
8. Yow, H.N.; Routh, A.F. Formation of liquid core-polymer shell microcapsules. *Soft Matter* **2006**, *2*(11), 940–949.
9. Rentschler, T. New approaches in papermaking with small particles. *Wochenbl Papierfabr* **2005**, *133*(22), 1385–1393.
10. El-Hennawi, H.M.; Ahmed, K.A.; Abd El-Thalouth, I. A novel bio-technique using laccase enzyme in textile printing to fix natural dyes. *Indian J. Fiber Text.* **2012**, *37*(3), 245–249.
11. Wataoka, I. Ink-jet printing using natural dyes. *J. Soc. Fiber Sci. Technol.* **2012**, *68*(6), 176–179 (in Japanese).
12. Thompson, D.W. *On Growth and Form*; Cambridge University Press: New York, 1961.
13. Burte, H.M.; Deussen, R.L.; Hemenger, P.M.; Hedberg, F.L. *The Potential Impact of Biotechnology on Composites*; Technomic Publishing: Lancaster, PA, 1986.

14. Beyer, M.; Koch, H.; Fischer, K. Role of hemicelluloses in the formation of chromophores during heat treatment of bleached chemical pulps. *Macromol. Symp.* **2006**, *232*, 98–106.
15. Fromageot, D.; Pichon, N.; Peyron, O.; Lemaire, J. Thermal yellowing sensitised by pre-photo-oxidation of non-deacidified paper Dominique Fromageot. *Polym. Degrad. Stabil.* **2006**, *91*, 347–357.
16. Chen, J.; Xie, J.; Wang, Y.; Meng, C.; Wu, G.; Zu, Q. Concept of heat-induced inkless eco-printing. *Carbohydr. Polym.* **2012**, *89*, 849–853.
17. Xie, J.; Chen, J.; Wang, Y.; Liu, Y.; Noori, M.N.; Pan, L. Weight Loss Phenomenon of paper and the mechanism for negligible damage of heat-induced inkless eco-printing. *Cell. Chem. Technol.* (in press).
18. Alava, M.; Niskanen, K. The physics of paper. *Rep. Prog. Phys.* **2006**, *69*, 669–723.
19. Mosier, N.; Wyman, C.; Dale, B.; Elander, R.; Lee, Y.Y.; Holtzapple, M.; et al. Features of promising technologies for pretreatment of lignocellulosic biomass. *Bioresour. Technol.* **2005**, *96*, 673–686.
20. Chen, G.; Li, C. Analysis and application on influencing factors of paper shrinkage rate. *China Pulp. Pap. Ind.* **2010**, *31*(20), 79–81 (in Chinese).
21. Carter, H.A. The chemistry of paper preservation: Part 2: The yellowing of paper and conservation bleaching. *J. Chem. Educ.* **1996**, *73*, 1068–1073.
22. Li, A.M.; Sun, L.J.; Li, R.D.; Wang, L. Characteristics of combustion and pyrolysis for decorative woods in poor-oxygen atmosphere. *J. Eng. Thermophys.* **2005**, *26* (s1), 237–240 (in Chinese).
23. Biagini, E.; Barontini, F.; Tognotti, L. Devolatilization of biomass fuels and biomass components studied by TG/FTIR technique. *Ind. Eng. Chem. Res.* **2006**, *45*, 4486–4493.
24. Elyoussi, K.; Blin, J.; Halim, M. High-yield charcoal production by two-step pyrolysis. *J. Anal. Appl. Pyrolysis.* **2010**, *87*, 138–143.
25. Tang, M.M.; Bacon, R. Carbonization of cellulose fibers low temperature pyrolysis. *Carbon.* **1964**, *2*, 211–220.
26. Fogassy, G.; Lorentz, C.; Toussaint, G.; Thegarid, N.; Schuurman, Y.; Mirodatos, C. Analytical techniques tailored for biomass transformation to biofuels. *Environ. Prog. Sustain.* **2013**, *32*(2), 377–383.
27. Demirbas, A. Mechanisms of liquefaction and pyrolysis reactions of biomass. *Energy Convers. Manag.* **2000**, *41*, 633–646.
28. Li, H.M.; Saeed, A.; Jahan, M.S.; Ni, Y.H.; Van Heiningen, A. Hemicellulose removal from hardwood chips in the pre-hydrolysis step of the kraft-based dissolving pulp production process. *J. Wood Chem. Technol.* **2010**, *30*(1), 48–60.
29. Arvelakis, S.; Jensen, P.A.; Dam-Johansen, M. Simultaneous thermal analysis (STA) on ash from high-alkali biomass. *Energ. Fuel* **2004**, *18*(4), 1066–1076.
30. Li, Y.P.; Wang, T.J.; Liang, W.; Wu, C.Z.; Ma, L.L.; Zhang, Q.; Zhang, X.H.; Jiang, T. Ultrasonic preparation of emulsions derived from aqueous bio-oil fraction and 0# diesel and combustion characteristics in diesel generator. *Energ. Fuel* **2010**, *24*, 1987–1995.
31. Dutta, B.; Raghavan, G.S.V.; Ngadi, M. Surface characterization and classification of slow and fast pyrolyzed biochar using novel methods of pycnometry and hyperspectral imaging. *J. Wood Chem. Technol.* **2012**, *32*(2), 105–120.
32. Milosavljevic, I.; Oja, V.; Suuberg, E.M. Thermal effects in cellulose pyrolysis: relationship to char formation processes. *Ind. Eng. Chem. Res.* **1996**, *35*(3), 653–662.
33. Yoshida, T.; Takano, T.; Kuroda, N. Thermal behavior of deteriorated wood waste. *J. Wood Chem. Technol.* **2011**, *31*(4), 298–308.
34. Wu, Y.M.; Zhao, Z.L.; Li, H.B.; He, F. Low temperature pyrolysis characteristics of major components of biomass. *J. Fuel Chem. Technol.* **2009**, *37*(4), 427–432 (in Chinese).